Pathogenic Tau Causes a Toxic Depletion of Nuclear Calcium

Rebekah Mahoney[1,2,3,6], **Elizabeth Ochoa Thomas**[1,2,3,6], **Paulino Ramirez**[1,2,3], **Henry E. Miller**[3,4], **Adrian Beckmann**[1,2,3], **Gabrielle Zuniga**[1,2,3], **Radek Dobrowolski**[2,5], **Bess Frost**[1,2,3,7,*]

[1]Barshop Institute for Longevity and Aging Studies, University of Texas Health, San Antonio, San Antonio, TX, USA

[2]Glenn Biggs Institute for Alzheimer's and Neurodegenerative Diseases, University of Texas Health, San Antonio, San Antonio, TX, USA

[3]Department of Cell Systems and Anatomy, University of Texas Health, San Antonio, San Antonio, TX, USA

[4]Greehey Children's Cancer Institute, University of Texas Health, San Antonio, San Antonio, TX, USA

[5]Rutgers University, Newark, NJ, USA

[6]These authors contributed equally

[7]Lead Contact

SUMMARY

Synaptic activity-induced calcium (Ca^{2+}) influx and subsequent propagation into the nucleus is a major way in which synapses communicate with the nucleus to regulate transcriptional programs important for activity-dependent survival and memory formation. Nuclear Ca^{2+} shapes the transcriptome by regulating cyclic AMP (cAMP) response element-binding protein (CREB). Here, we utilize a *Drosophila* model of tauopathy and induced pluripotent stem cell (iPSC)-derived neurons from humans with Alzheimer's disease to study the effects of pathogenic tau, a pathological hallmark of Alzheimer's disease and related tauopathies, on nuclear Ca^{2+}. We find that pathogenic tau depletes nuclear Ca^{2+} and CREB to drive neuronal death, that CREB-regulated genes are over-represented among differentially expressed genes in tau transgenic *Drosophila*, and that activation of big potassium (BK) channels elevates nuclear Ca^{2+} and suppresses tau-induced neurotoxicity. Our studies identify nuclear Ca^{2+} depletion as a mechanism contributing to tau-

*Correspondence: bfrost@uthscsa.edu.

induced neurotoxicity, adding an important dimension to the calcium hypothesis of Alzheimer's disease.

Graphical Abstract
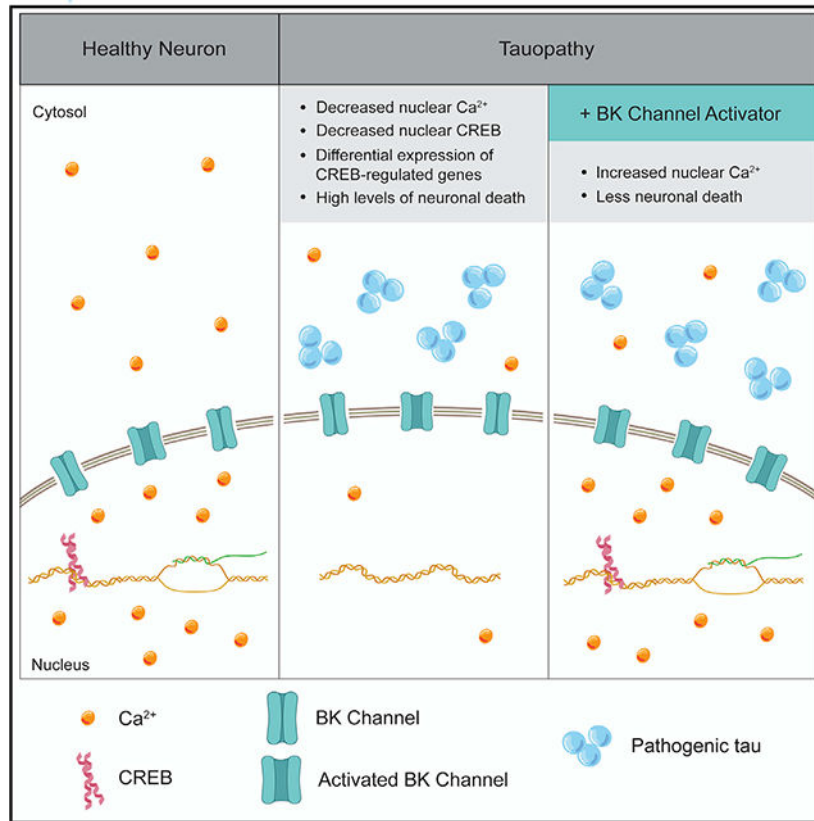
In Brief

Nuclear calcium (Ca^{2+}) is a major mediator of communication between synapses and nuclei and is critical for CREB-dependent gene expression. Mahoney et al. identify nuclear Ca^{2+} depletion as a pathomechanism connecting disease-associated forms of tau to neuronal death, adding an important dimension to the long-standing Ca^{2+} hypothesis of Alzheimer's disease.

INTRODUCTION

As a central signaling transducer, Ca^{2+} is integral to basic neuronal processes including membrane excitability and neuro-transmitter release from the synapse. In the nucleus, Ca^{2+} activates kinases that phosphorylate and thus activate CREB (Hardingham et al., 2001), a major transcriptional regulator of cellular programs critical for neuronal survival, plasticity, learning, and memory (Benito and Barco, 2010).

The long-standing "calcium hypothesis of Alzheimer's disease" posits that Ca^{2+} dyshomeostasis is a major mediator of neuronal deterioration (Khachaturian, 1984). Neuropatho-logically, Alzheimer's disease is defined by the presence of amyloid β plaques

and neurofibrillary tau tangles in postmortem human brain samples (Braak and Braak, 1991). Although a significant decrease in CREB and pCREB levels has been reported in postmortem human Alzheimer's disease brain tissue (Bartolotti et al., 2016; Bjorklund et al., 2012; Pugazhenthi et al., 2011), in primary hippocampal neurons from tau transgenic mice (Yin et al., 2016), and in β amyloid-based mouse models of Alzheimer's disease (Gong et al., 2004; Pugazhenthi et al., 2011), no study to date has investigated nuclear Ca^{2+} in the context of Alzheimer's disease and related tauopathies despite the well-established connection between nuclear Ca^{2+} and CREB activation (Hardingham et al., 2001).

To study potential links between pathogenic forms of tau and nuclear Ca^{2+}, we utilized a *Drosophila* model of tauopathy and induced pluripotent stem cell (iPSC)-derived neurons from patients with sporadic Alzheimer's disease. We selected a *Drosophila* model carrying a human tau transgene harboring the *R406W* disease-associated mutation (Wittmann et al., 2001). Tau[R406W] is one of many mutations in the *microtubule-associated protein tau* (*MAPT*) gene that cause an autosomal dominant neurological disorder termed frontotemporal lobar degeneration (FTLD)-tau with *MAPT* mutation (Forrest et al., 2018; Hutton et al., 1998). In *Drosophila*, similar mechanisms of tau-induced toxicity are shared by transgenic expression of various disease-associated tau mutations, which model human FTLD-tau with *MAPT* mutation, and wild-type human tau, which models Alzheimer's disease-associated tauopathy and other primary tauopathies not attributable to *MAPT* mutation (Bardai et al., 2018). The tau[R406W] *Drosophila* model has been used widely to study tau biology due to its mild toxicity at day 10 of adulthood, which is convenient for genetic analyses and precedes exponential decline in survival. To determine if our findings in tau[R406W] transgenic *Drosophila* were relevant to the wider group of human tauopathies that involve pathogenic forms of wild-type tau, we extended our studies to iPSC-derived neurons from patients with sporadic Alzheimer's disease.

We report that panneuronal expression of human tau[R406W] in the adult *Drosophila* brain is sufficient to deplete nuclear CREB protein levels, suggesting that pathogenic forms of tau may contribute to the previously reported nuclear depletion of CREB/pCREB in neurons of post-mortem human Alzheimer's disease brains (Bartolotti et al., 2016; Bjorklund et al., 2012; Pugazhenthi et al., 2011). We find that genes previously identified as CREB-regulated are over-represented among transcripts that are depleted in tau[R406W] transgenic *Drosophila*, suggesting that tau-induced CREB reduction significantly affects the transcriptome. We look upstream of CREB to find that both resting levels of nuclear Ca^{2+} and KCl-induced influx of nuclear Ca^{2+} are reduced as a result of human tau[R406W] expression in the adult *Drosophila* brain. We find that nuclear Ca^{2+} influx in response to membrane depolarization is also blunted in iPSC-derived neurons from patients with sporadic Alzheimer's disease, suggesting that our studies in *Drosophila* are relevant to sporadic human tauopathies that involve pathogenic forms of wild-type tau. Finally, our studies in *Drosophila* identify the BK channel as a pharmacologically targetable modifier of nuclear Ca^{2+} signaling and neuronal death in tauopathy. Taken together, our findings highlight a key role for nuclear Ca^{2+} and CREB depletion in the pathogenesis of Alzheimer's disease and related tauopathies.

RESULTS

Pathogenic Tau^{R406W} Induces Nuclear CREB Depletion in Neurons of the Adult *Drosophila* Brain

Previous studies report that levels of total and nuclear CREB and pCREB are reduced in postmortem human Alzheimer's disease brains (Bartolotti et al., 2016; Bjorklund et al., 2012; Pugazhenthi et al., 2011). To determine if pathogenic forms of tau can contribute to nuclear CREB depletion, we utilized a well-described *Drosophila* model of tauopathy (Wittmann et al., 2001). Transgenic expression of human tau^{R406W} in *Drosophila* neurons recapitulates many aspects of human Alzheimer's disease and related tauopathies including the degeneration of synapses (Merlo et al., 2014), ectopic cell cycle activation (Khurana et al., 2006), DNA damage (Frost et al., 2014; Khurana et al., 2012), and progressive neuronal death (Khurana et al., 2006; Wittmann et al., 2001).

To directly quantify the effects of pathological tau on the *Drosophila* homolog of human CREB, CrebB (Usui et al., 1993; Yin et al., 1995) (referred to throughout as "CREB" for simplicity), we performed western blotting on lysates from tau^{R406W} transgenic *Drosophila* heads at day 10 of adulthood, an age at which neurodegeneration is detectable, but prior to exponential decline in lifespan (Frost et al., 2016). Using an antibody that detects all CREB isoforms, we find that total CREB levels are depleted in heads of tau^{R406W} transgenic *Drosophila* versus controls (Figure 1A). We next directly visualized CREB localization by co-staining control and tau^{R406W} *Drosophila* brains with antibodies detecting CREB and elav, a protein restricted to neuronal nuclei. Similar to previous reports in postmortem human brains with Alzheimer's disease (Bartolotti et al., 2016; Bjorklund et al., 2012; Pugazhenthi et al., 2011), we find that total CREB (Figure 1B) and nuclear CREB (Figure 1C) are significantly depleted in brains of adult tau^{R406W} transgenic *Drosophila*.

CREB-Regulated Genes Are Over-Represented among Differentially Expressed Genes in Tau^{R406W} Transgenic *Drosophila*

As CREB is a transcription factor that is depleted in tau^{R406W} transgenic *Drosophila*, we next determined if CREB-regulated genes are over-represented among transcripts that are differentially expressed in brains of tau^{R406W} transgenic *Drosophila*. Genes that harbor a CREB-response element (CRE) between 3,000 bp upstream and 500 bp downstream of their transcription start site that have previously been identified as CREB targets based on chromatin immunoprecipitation sequencing (ChIP-seq) (Hirano et al., 2016; Data S1) were considered "CREB-regulated." The antibody used for ChIP-seq recognizes both activating and repressive isoforms of *Drosophila* CREB (Hirano et al., 2016). Genes that are differentially expressed between control and tau^{R406W} transgenic *Drosophila* at day 10 of adulthood were identified by RNA sequencing (Data S2). A hypergeometric test indicated that CREB-regulated genes are significantly over-represented among genes that are upregulated (1.84-fold enrichment, p = 3.77E–06) and downregulated (1.55-fold enrichment, p = 0.00046) in tau^{R406W} transgenic *Drosophila* compared to control (Data S3, gene list and Gene Ontology [GO] analysis). Although we cannot conclude that differential expression of these genes is a direct consequence of CREB depletion, this finding is consistent with the hypothesis that tau^{R406W}-induced CREB depletion significantly affects the transcriptome.

Physiological Aging and Tau^{R406W} Cause a Toxic Depletion of Nuclear Ca^{2+} in the *Drosophila* Brain

Given the dependence of CREB-mediated transcription on the presence of nuclear Ca^{2+} (Hardingham et al., 2001), we next determined the effect of pathological tau^{R406W} on nuclear Ca^{2+} using a GFP-based genetically encoded Ca^{2+} indicator fused to a nuclear localization signal, GCaMP3.NLS (Weislogel et al., 2013). Upon binding to Ca^{2+}, genetically encoded Ca^{2+} indicators undergo a conformational change that induces fluorescence (Nakai et al., 2001). We focused specifically on the cells of the mushroom body of the adult fly brain, as activation of the nuclear Ca^{2+} reporter can be visualized in this brain region in living flies (Weislogel et al., 2013; Figure 2A), and the mushroom body is central to *Drosophila* learning and memory (Heisenberg, 2003). *In vivo* confocal imaging reveals that tau^{R406W} transgenic *Drosophila* have significantly lower resting levels of nuclear Ca^{2+} in the cells of the mushroom body compared to controls at day 10 of adulthood (Figure 2B). Importantly, we found that decreased nuclear Ca^{2+} levels are not simply a result of extensive neuronal loss (Figure S1A). As an important control, we confirmed that transgenic human tau^{R406W} does not affect expression levels of the genetically encoded Ca^{2+} indicator itself (Figure S1B).

To determine if tau^{R406W}-induced nuclear Ca^{2+} depletion is age-dependent, we quantified resting levels of nuclear Ca^{2+} at day 1, 10, and 30 of adulthood in control and tau^{R406W} transgenic *Drosophila*. We extended our analysis to 60 days in control flies, which is close to their maximum lifespan of ~70 days, and exceeds the maximum lifespan of tau^{R406W} transgenic *Drosophila* of ~35 days (Frost et al., 2016). In both genotypes, we find a significant age-dependent decrease in levels of resting nuclear Ca^{2+} (Figures S1C and S1D). Although nuclear Ca^{2+} levels do not significantly differ between control and tau^{R406W} transgenic *Drosophila* at day 1 of adulthood, we find that tau^{R406W} transgenic *Drosophila* have reduced levels of nuclear Ca^{2+} compared to controls at days 10 and 30 (Figure 2C), indicating that tau^{R406W} exacerbates the depletion of resting nuclear Ca^{2+} levels that occurs with normal aging.

To determine if depletion of nuclear Ca^{2+} signaling is causally associated with neurodegeneration, we overexpressed a recombinant blocker of nuclear Ca^{2+}, CaMBP4 (Weislogel et al., 2013), in neurons of the adult *Drosophila* brain. CaMBP4 is a nuclear protein that contains four copies of a calmodulin-binding peptide (M13). CaMBP4 binds to and inactivates Ca^{2+}-bound calmodulin complexes, thus blocking activation of Ca^{2+}-dependent nuclear signaling cascades. Although blocking nuclear Ca^{2+}-dependent processes via CaMBP4 overexpression is not sufficient to induce neuronal death at day 10 of adulthood based on terminal deoxynucleotidyl transferase dUTP nick end labeling (TUNEL), we find that genetically blocking nuclear Ca^{2+} signaling in tau^{R406W} transgenic *Drosophila* significantly enhances tau^{R406W}-induced neuronal death (Figure 2D). Taken together, these data suggest that tau^{R406W}-induced decrease in nuclear Ca^{2+} signaling is causally associated with neurodegeneration.

Decreased Influx of Nuclear Ca^{2+} in Tau^{R406W} Transgenic *Drosophila* and iPSC-Derived Neurons from Sporadic Human Alzheimer's Disease Patients in Response to Membrane Depolarization

Ca^{2+} is a central regulator of communication between the synapse and nucleus, and Ca^{2+} that enters the nucleus in response to synaptic activity mediates memory formation (Bading, 2013). Having established that resting levels of nuclear Ca^{2+} are depleted as a consequence of pathogenic tau^{R406W}, we next determined if influx of Ca^{2+} into the nucleus is affected in tauopathy when the membrane is induced to depolarize. We quantified nuclear Ca^{2+} upon *in vivo* brain exposure to 70 mM KCl, which induces membrane depolarization and opening of voltage-gated Ca^{2+} channels (Fiala and Spall, 2003). After normalizing to resting nuclear Ca^{2+} levels, we find that KCl-induced nuclear Ca^{2+} influx is significantly depleted in brains of tau^{R406W} transgenic *Drosophila* at day 10 of adulthood compared to control (Figures 3A and 3B). Together with our previous findings, these data indicate that both resting levels and membrane depolarization-induced nuclear Ca^{2+} influx are depleted as a consequence of pathogenic tau^{R406W}.

We next utilized iPSC-derived neurons from patients with sporadic Alzheimer's disease to determine if our findings were relevant to a human tauopathy that involves pathogenic forms of wild-type tau. As in brains of patients with Alzheimer's disease, iPSC-derived neurons from patients with Alzheimer's disease are reported to feature disease-associated tau phosphorylation (Israel et al., 2012; Ochalek et al., 2017). After differentiating iPSCs into excitatory forebrain neurons (Chambers et al., 2009; Reddy et al., 2016; Sproul et al., 2014), we quantified membrane depolarization-induced changes in nuclear Ca^{2+} levels using a GCaMP6s.NLS genetically encoded nuclear Ca^{2+} sensor (Hagenston and Bading, 2011). We do not observe differences in differentiation status between iPSC-derived neurons from control and Alzheimer's disease patients (Figure S2). We find that KCl-induced increase of nucleoplasmic Ca^{2+} is reduced in iPSC-derived neurons from three different sporadic cases of human Alzheimer's disease versus controls (Figures 3C and 3D), suggesting that the blunting of KCl-induced nuclear Ca^{2+} influx detected in tau^{R406W} transgenic *Drosophila* is relevant to human Alzheimer's disease and is not restricted to the *R406W* tau mutation.

Manipulation of BK Channels Modifies Tau^{R406W}-Induced Nuclear Ca^{2+} Reduction and Neurotoxicity

We became interested in BK channels as a potential mechanistic link between pathogenic tau and nuclear Ca^{2+} depletion based on a previous study reporting that BK channels regulate induced release of Ca^{2+} from nuclear envelope stores (Li et al., 2014). We find that oral administration of a potent activator of BK channels, BMS-191011, significantly increases resting levels of nuclear Ca^{2+} in cells of the mushroom body of the adult tau^{R406W} transgenic *Drosophila* brain (Figures 4A and 4B). In addition, we find that BMS-191011 significantly reduces neurodegeneration in tau^{R406W} transgenic *Drosophila* at day 10 of adulthood (Figure 4C).

Having established that manipulation of BK channels is sufficient to increase nuclear Ca^{2+} and suppress neurodegeneration in tau^{R406W} transgenic *Drosophila*, we next determined if genetic depletion of the *Drosophila* BK channel homolog, *slowpoke*, enhances tau^{R406W}-

induced neurodegeneration. We decreased slowpoke activity by RNAi-mediated reduction (slo^{RNAi}) or introduction of a heterozygous loss-of-function mutation (slo^1). Although neither genetic manipulation is sufficient to induce neuronal death based on TUNEL staining at day 10 of adulthood, we find that both slo^{RNAi} and slo^1 significantly enhance tau^{R406W}-induced neuronal death (Figure 4D). Taken together, these data suggest that manipulation of BK channels can modify tau^{R406W}-induced nuclear Ca^{2+} reduction and consequent neuronal death.

DISCUSSION

In the current study, we investigate the effects of pathogenic tau on nuclear Ca^{2+} and CREB. Our studies suggest that pathogenic tau directly contributes to CREB depletion, as we find that panneuronal expression of human transgenic tau^{R406W} in the adult *Drosophila* brain is sufficient to reduce total and nuclear levels of CREB protein. Based on RNA sequencing, we detect a significant over-representation of CREB-regulated genes among transcripts that are differentially expressed in tau^{R406W} transgenic *Drosophila* compared to control. As differential splicing produces both activating and repressive CREB isoforms in *Drosophila* (Yin et al., 1995), the overrepresentation of CREB-regulated genes that are both up- and downregulated in tau^{R406W} transgenic *Drosophila* is not unexpected. Although these data are consistent with the role of CREB as a key cellular transcription factor, additional studies are required to determine if the transcriptional changes in tau^{R406W} transgenic *Drosophila* are a direct result of CREB depletion.

Based on the dependence of CREB activation on nuclear Ca^{2+}, we then visualized nuclear Ca^{2+} levels in neurons of live *Drosophila* brains using a genetically encoded, nuclear-localized Ca^{2+} indicator. The ability to quantify nuclear Ca^{2+} levels as a function of biological aging is an advantage of the *Drosophila* system. We found that resting-state nuclear Ca^{2+} levels are depleted with physiological aging, and that pathogenic tau^{R406W} significantly exacerbates age-associated nuclear Ca^{2+} depletion. We found that genetic blockage of nuclear Ca^{2+} signaling further enhances tau^{R406W}-induced neuronal death, suggesting that nuclear Ca^{2+} depletion is a causal mediator of neurodegeneration in tauopathy.

As generation of nuclear Ca^{2+} transients are a key route of communication between synapses and nuclei, we next asked if KCl-induced nuclear Ca^{2+} influx is depleted in the context of tauopathy. Using tau^{R406W} transgenic *Drosophila* as well as iPSC-derived neurons from patients with sporadic Alzheimer's disease, we find that the nuclear Ca^{2+} response to KCl-induced depolarization is blunted in both model systems. Our studies in tau^{R406W} transgenic *Drosophila* and in human Alzheimer's disease iPSC-derived neurons suggest that depletion of nuclear Ca^{2+} is neither specific to the *Drosophila* system nor *R406W* mutant tau.

We identify BK channels as a potential pharmacologically targetable link between pathogenic tau and nuclear Ca^{2+} depletion. Treatment of tau^{R406W} transgenic *Drosophila* with a BK channel activator increases nuclear Ca^{2+} levels and suppresses tau^{R406W} neurotoxicity, while genetically depleting BK channels significantly enhances tau^{R406W}

neurotoxicity. A previous study has reported that BK channels are present in the nuclear envelope and regulate nuclear Ca^{2+} levels, nuclear Ca^{2+} signaling, and activity-evoked gene expression (Li et al., 2014). While we cannot rule out the possibility that BK channels on the plasma membrane contribute to nuclear Ca^{2+} regulation in neurons of tau[R406W] transgenic *Drosophila*, we would expect that activation of BK channels on the plasma membrane would hyperpolarize the membrane, preventing further Ca^{2+} influx into the cytoplasm. We thus speculate that nuclear envelope-localized BK channels, rather than plasma membrane-localized BK channels, are the primary contributor to nuclear Ca^{2+} depletion in tauopathy by influencing Ca^{2+} stores in the nuclear envelope.

Pharmacological blockade of nuclear BK channels was previously reported to elevate nuclear Ca^{2+} in isolated neuronal nuclei and in cultured mouse hippocampal neurons (Li et al., 2014), which conflicts with our finding that that activation of BK channels elevates nuclear Ca^{2+} in brains of tau[R406W] transgenic *Drosophila*. Several differences between our respective experimental designs may underlie the discrepancy between studies. First, Li et al. (2014) analyzed nuclear Ca^{2+} in isolated nuclei and cultured neurons, whereas our live-imaging measurements of nuclear Ca^{2+} utilize intact *Drosophila* brains. Second, we analyzed levels of resting nuclear Ca^{2+} in tau[R406W] transgenic *Drosophila* in response to chronic exposure to the BK channel activator throughout adulthood, whereas Li et al. (2014) measured nuclear Ca^{2+} influx in response to transient BK channel blockage. Despite divergent findings between the two studies, both point toward a critical role of BK channels as a regulator of nuclear Ca^{2+}. Our study is consistent with that of Wang et al. (2015a, 2015b), who find that drug-induced BK channel activation suppresses cognitive deficits in the 3xTg mouse model of Alzheimer's disease, which harbors *APP*, *PS1*, and *MAPT* disease-associated mutant human transgenes (Oddo et al., 2003).

Why might depletion of nuclear Ca^{2+} be toxic to neurons? In addition to regulating a neuroprotective genetic program consisting of synaptic activity-induced "activity-regulated inhibitor of death" genes (Zhang et al., 2009), nuclear Ca^{2+} has been identified as a key regulator of the autolysosomal system (Reddy et al., 2016). As the autophagy-lysosome system is clearly dysfunctional in tauopathy (Uddin et al., 2018), determining the effects of tau-induced nuclear Ca^{2+} depletion on protein clearance pathways is an important avenue of investigation for future studies.

In summary, our study provides insight into the effects of pathogenic tau on nuclear Ca^{2+}, which is a major mediator of communication between synapses and nuclei (Bading, 2013) and regulator of protein clearance pathways (Reddy et al., 2016). We identify nuclear Ca^{2+} depletion as a pathomechanism connecting disease-associated forms of tau to neuronal death, adding an important dimension to the long-standing Ca^{2+} hypothesis of Alzheimer's disease.

STAR★ METHODS

RESOURCE AVAILABILITY

Lead Contact—Further information and requests for resources and reagents should be directed to and will be fulfilled by the Lead Contact, Dr. Bess Frost (bfrost@uthscsa.edu).

Materials Availability—This study did not generate new unique reagents.

Data and Code Availability—The accession number of the raw RNA-seq files for *Drosophila* control versus tau[R406W] transgenic *Drosophila* reported in this paper is GEO: GSE152278.

EXPERIMENTAL MODEL AND SUBJECT DETAILS

Drosophila genetics and models—All *Drosophila melanogaster* crosses and aging were performed at 25°C on a 12-hour light/dark cycle. Males and females of indicated genotypes were housed in the same vial, and each experiment utilized an equal number of male and female flies. Food was made fresh weekly and flies were transferred to fresh food every two days. Transgenic flies harboring human tau[R406W] have been described previously (Wittmann et al., 2001). Panneuronal expression of transgenes or RNAi small hairpins were achieved using the Gal4/UAS system with the *elav* promoter driving expression of the Gal4 transcription factor. UAS-slo[RNAi] and slo[1] were obtained from the Bloomington *Drosophila* Stock Center. UAS-GCaMP3.NLS and CaMBP4 transgenic flies were generously provided by Dr. Hilmar Bading (Weislogel et al., 2013).

iPSC-derived neurons—iPSCs from sporadic Alzheimer's disease patients (no *ApoE4* carriers) and control lines were obtained from the Coriell Institute (Camden, NJ). Neural progenitor cells were derived following established protocols (Chambers et al., 2009) and differentiated into forebrain neurons by stepwise addition (daily half-feeds for one week) of neurodifferentiation media composed of Neurobasal Medium supplemented with B-27 minus retinoic acid, Glutamax and Pen/Strep as described (Reddy et al., 2016; Sproul et al., 2014). The resulting excitatory forebrain neurons are cultured for another three weeks to allow further differentiation, which is monitored by expression of neuronal markers including MAP2 and vGluT1 (Figure S2).

METHOD DETAILS

RNA sequencing and analysis—6 biologically independent replicates were sequenced per genotype, each consisting of 15–30 ng of total RNA from 18 pooled *Drosophila* heads (108 heads per genotype in total). Trizol-extracted RNA was used for library preparation using the Ovation RNA-Seq System for *Drosophila* according to the User Guide. After quantification by Qubit and bioanalysis, libraries were pooled, purified by magnetic bead extraction and sequenced on the Illumina HiSeq 3000 platform with 100 base pair paired-end sequencing. Library quality control and RNA-sequencing was performed by the Genome Sequencing Facility at Greehey Children's Cancer Research Institute at the University of Texas Health San Antonio.

Raw FASTQ files underwent quality control and were trimmed with Trimmomatic v.0.36 (Bolger et al., 2014) to remove adapters and low-quality reads. FastQC (http://www.bioinformatics.babraham.ac.uk/projects/fastqc/) was used to evaluate the quality of the reads before and after trimming. Trimmed FASTQ files were mapped and aligned to the *Drosophila melanogaster* transcriptome (FlyBase (Thurmond et al., 2019) FB2018_6.27) using Salmon v.0.13.1 (Patro et al., 2017). Differential expression analysis was performed

using DESeq2 v1.24 (Love et al., 2014). Genes with an adjusted p value of less than 0.05 were considered significant.

CRE and CREB binding-site analyses—Genes harboring a CRE were identified through the FindM program (Ambrosini et al., 2003; Bucher and Trifonov, 1986). The canonical full CRE site and the CRE half site were included. One mismatch was allowed for full sites, and no mismatches were allowed for half sites. CRE prediction sites that were between 3,000 bp upstream and 500 bp downstream of annotated genomic transcription start sites were utilized in subsequent analyses.

To validate predicted CREB target sites, CREB ChIP-seq data were downloaded from the Gene Expression Omnibus (GEO: GSE73386, samples GSM1892406 and GSM1892408) (Edgar et al., 2002; Hirano et al., 2016) and compared to predicted CRE sites. Files were converted into GRanges format and annotated with ChIPpeakAnno (Zhu et al., 2010). CREB ChIP-seq peaks that did not fall between 3,000 bp upstream and 500 bp downstream of an annotated TSS were discarded. The intersection between FindM-based CRE-containing genes, ChIP-seq-based CREB-bound genes, and genes that were up and downregulated in tau^{R406W} transgenic *Drosophila* compared to control (adjusted p < 0.05) were extracted. A hypergeometric test was used to determine enrichment of CRE-containing, CREB-regulated genes in the lists of up and downregulated genes. GO analysis was performed on the CRE-containing, CREB-regulated genes that were up and downregulated in tau^{R406W} transgenic *Drosophila* using the GO Enrichment Analysis tool (Ashburner et al., 2000), which utilizes the *Drosophila melanogaster* genome as a background gene set (Data S3). GO annotations with a false discovery rate (FDR) of less than 0.05 were considered significant.

Ca^{2+} imaging—To quantify resting nuclear Ca^{2+} levels in brains of living flies (Figures 2A–2C, 4A, and 4B), a single fly was placed on a CO$_2$ gas pad until the fly lost postural control, then transferred into a 100% ethanol bath for 10 s. Using a small Sylgard dissection surface, the fly was then placed in cold HL3 solution (70 mM NaCl, 5 mM KCl, 10 mM NaHCO$_3$, 5 mM trehalose, 115 mM sucrose, 5 mM HEPES, 0.5 mM CaCl$_2$, 3 mM MgCl$_2$) and pinned using modified minutien pins on its ventral surface (Mahoney et al., 2014). Once positioned, a small piece of cuticle was removed from the posterior side of the head (cuticular window) to reveal the underlying mushroom body (Weislogel et al., 2013). GFP fluorescence resulting from GCaMP3.NLS activation was imaged with a Zeiss LSM 780 NLO with Examiner. ImageJ was used for analysis. Six biological replicates were analyzed per group.

To quantify the nuclear Ca^{2+} response to KCl-induced membrane depolarization (Figures 3A and 3B), flies were first prepared for imaging in a cold HL3 solution as described above, and resting GCaMP3.NLS fluorescence levels were recorded. HL3 was removed from the exposed fly brain by pipetting and was immediately replaced with a modified HL3 solution containing 70 mM KCl. GCaMP3.NLS reporter intensity stabilizes a few seconds after KCl exposure, as flies experience some movement within the imaging system as a result of the physical administration of the buffer. After a three second recovery, baseline intensity was set to one for both control and tau^{R406W} transgenic *Drosophila*. The KCl-induced nuclear

Ca^{2+} response is presented as change from baseline (Weislogel et al., 2013). Six biological replicates were analyzed per group.

In iPSC-derived neurons, nuclear Ca^{2+} levels were measured using the human *Synapsin 1* promoter-driven GCaMP6s.NLS (Hagenston and Bading, 2011), ensuring expression exclusively in neurons. This genetically encoded nuclear Ca^{2+} reporter was transfected into iPSC-derived human neurons using BioT. To assess transfection efficiency and simplify visualization of transfected cells during the experiment, cells were co-transfected with membrane-RFP (mRFP) in addition to GCaMP6s.NLS. While mRFP labels all transfected cells, GCaMP6s.NLS fluorescence is restricted to neurons and is induced following KCl-mediated depolarization. mTagRFP-Membrane-1 was a gift from Michael Davidson (Addgene plasmid #57992).

Baseline fluorescence and KCl (25 mM)-induced GCaMP6s.NLS fluorescence were measured by spinning disc confocal microscopy over time, and peak fluorescence intensities were recorded. Minima and maxima intensities were normalized to 0 or 1, respectively. Data are presented as peak $\Delta F/F_0$, in which ΔF is the change in fluorescence and F_0 is baseline fluorescence. Cells with saturating F_0 fluorescence are excluded from experimental measurements. To avoid measuring nuclear Ca^{2+} in cells that have no or very low expression of the GCaMP6s.NLS nuclear Ca^{2+} indicator, the microscopy field of view is set such that all cells within the field of view exhibit a baseline GFP signal. $\Delta F/F_0$ peak values presented in Figure 3D represent the maximum values of longitudinal measurements ($\Delta F/F_0$ over time). Longitudinal measurements did not plateau at their maxima at any point in time, indicating that the signal was not saturated. A technical replicate consists of the average signal from at least 50 single cells derived from one patient sample. There were six technical replicates assayed per patient-derived sample, with two biologically distinct control samples and three biologically distinct sporadic Alzheimer's disease samples.

Drug Preparation—BMS 191011 was prepared as a stock solution in ethanol and diluted in fly food to a final concentration of 20 μM. Vehicle-treated flies were reared on food containing an equivalent volume of ethanol. Flies were treated from day 2–10 of adulthood.

Western blotting—Frozen *Drosophila* heads were homogenized in 20 μL 2X Laemmli sample buffer, boiled for 10 min, and run on a 4%–20% SDS-PAGE gel. Equal loading of protein was assessed by Ponceau S staining prior to blotting. After blocking membranes in PBS plus 0.05% Tween (PBS_{TW}) and 2% milk, membranes were incubated with primary antibodies overnight at 4°C. After washing in PBS_{TW}, membranes were incubated with their respective HRP-conjugated secondary antibodies for 2 hr at room temperature. Blots were developed with Clarity Max ECL Western Blotting Substrate. Band intensity was quantified with ImageJ. Antibodies against actin and GFP were used at 1:10,000 for western blotting, and CREB was used at 1:500.

Immunofluorescence and histology—For *Drosophila* studies, *Drosophila* brains were dissected in PBS and fixed in methanol for 20 min. After blocking with 2% milk PBS_{Tr} for 30 minutes, brains were incubated with primary antibody diluted in blocking solution overnight at 4°C. After washing with PBS_{Tr}, brains were incubated with Alexa488- or

Alexa555-conjugated secondary antibodies for 2 hr at room temperature in 2% milk dissolved in PBS_T. Slides were washed with PBS_{Tr} and then incubated with DAPI for 2 minutes to visualize nuclei. Brains were imaged by confocal microscopy (Zeiss LSM 780 NLO with Examiner). ImageJ was used for analysis. For quantification of neuronal nuclear CREB in *Drosophila*, dissected brains were fixed in 100% methanol and stained with antibodies detecting *Drosophila* CREB and elav (1:100 and 1:5, respectively). Elav-based masks were created in ImageJ and CREB fluorescence within the elav-positive area was quantified in six control and six tau^{R406W} transgenic dissected *Drosophila* brains.

TUNEL staining was performed on 4 μm sections of formalin-fixed, paraffin embedded *Drosophila* heads. Secondary identification of TUNEL-positive nuclei was performed using DAB. TUNEL-positive nuclei were counted throughout the entire brain by bright field microscopy.

QUANTIFICATION AND STATISTICAL ANALYSIS

A Student's t test was used for all pairwise comparisons. A one-way ANOVA using a Tukey multiple comparisons test (alpha = 0.05) was used to compare all multiple values. For all statistical analyses, a confidence interval of 95% and normal distribution were assumed. For *in vivo Drosophila* experiments (Figures 1, 2, 3A, 3B, and 4), each biological replicate is one *Drosophila* brain. For *in vitro* iPSC-derived neuron experiments (Figures 4C and D), each biological replicate is one biologically distinct patient-derived cell population. Statistical analysis was performed using Prism8. Statistical details can be found in the figure legends and text, where appropriate.

Supplementary Material

Refer to Web version on PubMed Central for supplementary material.

ACKNOWLEDGMENTS

REFERENCES

Ambrosini G, Praz V, Jagannathan V, and Bucher P (2003). Signal search analysis server. Nucleic Acids Res. 31, 3618–3620. [PubMed: 12824379]

Ashburner M, Ball CA, Blake JA, Botstein D, Butler H, Cherry JM, Davis AP, Dolinski K, Dwight SS, Eppig JT, et al.; The Gene Ontology Consortium (2000). Gene ontology: tool for the unification of biology. Nat. Genet 25, 25–29. [PubMed: 10802651]

Bading H (2013). Nuclear calcium signalling in the regulation of brain function. Nat. Rev. Neurosci 14, 593–608. [PubMed: 23942469]

Bardai FH, Wang L, Mutreja Y, Yenjerla M, Gamblin TC, and Feany MB (2018). A Conserved Cytoskeletal Signaling Cascade Mediates Neurotoxicity of FTDP-17 Tau Mutations *In Vivo*. J. Neurosci 38, 108–119. [PubMed: 29138281]

Bartolotti N, Bennett DA, and Lazarov O (2016). Reduced pCREB in Alzheimer's disease prefrontal cortex is reflected in peripheral blood mononuclear cells. Mol. Psychiatry 21, 1158–1166. [PubMed: 27480489]

Benito E, and Barco A (2010). CREB's control of intrinsic and synaptic plasticity: implications for CREB-dependent memory models. Trends Neurosci 33, 230–240. [PubMed: 20223527]

Bjorklund NL, Reese LC, Sadagoparamanujam VM, Ghirardi V, Woltjer RL, and Taglialatela G (2012). Absence of amyloid b oligomers at the post-synapse and regulated synaptic Zn2+ in cognitively intact aged individuals with Alzheimer's disease neuropathology. Mol. Neurodegener 7, 23. [PubMed: 22640423]

Bolger AM, Lohse M, and Usadel B (2014). Trimmomatic: a flexible trimmer for Illumina sequence data. Bioinformatics 30, 2114–2120. [PubMed: 24695404]

Braak H, and Braak E (1991). Neuropathological stageing of Alzheimer-related changes. Acta Neuropathol. 82, 239–259. [PubMed: 1759558]

Bucher P, and Trifonov EN (1986). Compilation and analysis of eukaryotic POL II promoter sequences. Nucleic Acids Res. 14, 10009–10026. [PubMed: 3808945]

Chambers SM, Fasano CA, Papapetrou EP, Tomishima M, Sadelain M, and Studer L (2009). Highly efficient neural conversion of human ES and iPS cells by dual inhibition of SMAD signaling. Nat. Biotechnol 27, 275–280. [PubMed: 19252484]

Edgar R, Domrachev M, and Lash AE (2002). Gene Expression Omnibus: NCBI gene expression and hybridization array data repository. Nucleic Acids Res. 30, 207–210. [PubMed: 11752295]

Fiala A, and Spall T (2003). In vivo calcium imaging of brain activity in Drosophila by transgenic cameleon expression. Sci. STKE 2003, PL6. [PubMed: 12644713]

Forrest SL, Kril JJ, Stevens CH, Kwok JB, Hallupp M, Kim WS, Huang Y, McGinley CV, Werka H, Kiernan MC, et al. (2018). Retiring the term FTDP-17 as MAPT mutations are genetic forms of sporadic frontotemporal tauopathies. Brain 141, 521–534. [PubMed: 29253099]

Frost B, Hemberg M, Lewis J, and Feany MB (2014). Tau promotes neurodegeneration through global chromatin relaxation. Nat. Neurosci 17, 357–366. [PubMed: 24464041]

Frost B, Bardai FH, and Feany MB (2016). Lamin Dysfunction Mediates Neurodegeneration in Tauopathies. Curr. Biol 26, 129–136. [PubMed: 26725200]

Gong B, Vitolo OV, Trinchese F, Liu S, Shelanski M, and Arancio O (2004). Persistent improvement in synaptic and cognitive functions in an Alzheimer mouse model after rolipram treatment. J. Clin. Invest 114, 1624–1634. [PubMed: 15578094]

Hagenston AM, and Bading H (2011). Calcium signaling in synapse-to-nucleus communication. Cold Spring Harb. Perspect. Biol 3, a004564. [PubMed: 21791697]

Hardingham GE, Arnold FJL, and Bading H (2001). Nuclear calcium signaling controls CREB-mediated gene expression triggered by synaptic activity. Nat. Neurosci 4, 261–267. [PubMed: 11224542]

Heisenberg M (2003). Mushroom body memoir: from maps to models. Nat. Rev. Neurosci 4, 266–275. [PubMed: 12671643]

Hirano Y, Ihara K, Masuda T, Yamamoto T, Iwata I, Takahashi A, Awata H, Nakamura N, Takakura M, Suzuki Y, et al. (2016). Shifting transcriptional machinery is required for long-term memory maintenance and modification in Drosophila mushroom bodies. Nat. Commun 7, 13471. [PubMed: 27841260]

Hutton M, Lendon CL, Rizzu P, Baker M, Froelich S, Houlden H, Pickering-Brown S, Chakraverty S, Isaacs A, Grover A, et al. (1998). Association of missense and 5^0-splice-site mutations in tau with the inherited dementia FTDP-17. Nature 393, 702–705. [PubMed: 9641683]

Israel MA, Yuan SH, Bardy C, Reyna SM, Mu Y, Herrera C, Hefferan MP, Van Gorp S, Nazor KL, Boscolo FS, et al. (2012). Probing sporadic and familial Alzheimer's disease using induced pluripotent stem cells. Nature 482, 216–220. [PubMed: 22278060]

Khachaturian Z (1984). Towards theories of brain aging In Handbook of Studies on Psychiatry and Old Age (Elsevier Science Publishers), pp. 7–30.

Khurana V, Lu Y, Steinhilb ML, Oldham S, Shulman JM, and Feany MB (2006). TOR-mediated cell-cycle activation causes neurodegeneration in a Drosophila tauopathy model. Curr. Biol 16, 230–241. [PubMed: 16461276]

Khurana V, Merlo P, DuBoff B, Fulga TA, Sharp KA, Campbell SD, Götz J, and Feany MB (2012). A neuroprotective role for the DNA damage checkpoint in tauopathy. Aging Cell 11, 360–362. [PubMed: 22181010]

Li B, Jie W, Huang L, Wei P, Li S, Luo Z, Friedman AK, Meredith AL, Han M-H, Zhu X-H, and Gao TM (2014). Nuclear BK channels regulate gene expression via the control of nuclear calcium signaling. Nat. Neurosci 17, 1055–1063. [PubMed: 24952642]

Love MI, Huber W, and Anders S (2014). Moderated estimation of fold change and dispersion for RNA-seq data with DESeq2. Genome Biol. 15, 550. [PubMed: 25516281]

Mahoney RE, Rawson JM, and Eaton BA (2014). An age-dependent change in the set point of synaptic homeostasis. J. Neurosci 34, 2111–2119. [PubMed: 24501352]

Merlo P, Frost B, Peng S, Yang YJ, Park PJ, and Feany M (2014). p53 prevents neurodegeneration by regulating synaptic genes. Proc. Natl. Acad. Sci. USA 111, 18055–18060. [PubMed: 25453105]

Nakai J, Ohkura M, and Imoto K (2001). A high signal-to-noise Ca(2+) probe composed of a single green fluorescent protein. Nat. Biotechnol 19, 137–141. [PubMed: 11175727]

Ochalek A, Mihalik B, Avci HX, Chandrasekaran A, Téglási A, Bock I, Giudice ML, Táncos Z, Molnár K, László L, et al. (2017). Neurons derived from sporadic Alzheimer's disease iPSCs reveal elevated TAU hyperphosphorylation, increased amyloid levels, and GSK3B activation. Alzheimers Res. Ther. 9, 90.

Oddo S, Caccamo A, Shepherd JD, Murphy MP, Golde TE, Kayed R, Metherate R, Mattson MP, Akbari Y, and LaFerla FM (2003). Triple-transgenic model of Alzheimer's disease with plaques and tangles: intracellular Abeta and synaptic dysfunction. Neuron 39, 409–421. [PubMed: 12895417]

Patro R, Duggal G, Love MI, Irizarry RA, and Kingsford C (2017). Salmon provides fast and bias-aware quantification of transcript expression. Nat. Methods 14, 417–419. [PubMed: 28263959]

Pugazhenthi S, Wang M, Pham S, Sze C-I, and Eckman CB (2011). Downregulation of CREB expression in Alzheimer's brain and in Ab-treated rat hippocampal neurons. Mol. Neurodegener 6, 60. [PubMed: 21854604]

Reddy K, Cusack CL, Nnah IC, Khayati K, Saqcena C, Huynh TB, Noggle SA, Ballabio A, and Dobrowolski R (2016). Dysregulation of Nutrient Sensing and CLEARance in Presenilin Deficiency. Cell Rep. 14, 2166–2179. [PubMed: 26923592]

Sproul AA, Jacob S, Pre D, Kim SH, Nestor MW, Navarro-Sobrino M, Santa-Maria I, Zimmer M, Aubry S, Steele JW, et al. (2014). Characterization and molecular profiling of PSEN1 familial Alzheimer's disease iPSC-derived neural progenitors. PLoS ONE 9, e84547. [PubMed: 24416243]

Thurmond J, Goodman JL, Strelets VB, Attrill H, Gramates LS, Mary-gold SJ, Matthews BB, Millburn G, Antonazzo G, Trovisco V, et al.; FlyBase Consortium (2019). FlyBase 2.0: the next generation. Nucleic Acids Res. 47 (D1), D759–D765. [PubMed: 30364959]

Uddin MS, Stachowiak A, Mamun AA, Tzvetkov NT, Takeda S, Atanasov AG, Bergantin LB, Abdel-Daim MM, and Stankiewicz AM (2018). Autophagy and Alzheimer's Disease: From Molecular Mechanisms to Therapeutic Implications. Front. Aging Neurosci 10, 04. [PubMed: 29441009]

Usui T, Smolik SM, and Goodman RH (1993). Isolation of Drosophila CREB-B: a novel CRE-binding protein. DNA Cell Biol. 12, 589–595. [PubMed: 8397816]

Wang F, Zhang Y, Wang L, Sun P, Luo X, Ishigaki Y, Sugai T, Yamamoto R, and Kato N (2015a). Improvement of spatial learning by facilitating large-conductance calcium-activated potassium channel with transcranial magnetic stimulation in Alzheimer's disease model mice. Neuropharmacology 97, 210–219. [PubMed: 26051398]

Wang L, Kang H, Li Y, Shui Y, Yamamoto R, Sugai T, and Kato N (2015b). Cognitive recovery by chronic activation of the large-conductance calcium-activated potassium channel in a mouse model of Alzheimer's disease. Neuropharmacology 92, 8–15. [PubMed: 25577958]

Weislogel J-M, Bengtson CP, Müller MK, Hörtzsch JN, Bujard M, Schuster CM, and Bading H (2013). Requirement for nuclear calcium signaling in Drosophila long-term memory. Sci. Signal 6, ra33. [PubMed: 23652205]

Wittmann CW, Wszolek MF, Shulman JM, Salvaterra PM, Lewis J, Hutton M, and Feany MB (2001). Tauopathy in Drosophila: neurodegeneration without neurofibrillary tangles. Science 293, 711–714. [PubMed: 11408621]

Yin JC, Wallach JS, Wilder EL, Klingensmith J, Dang D, Perrimon N, Zhou H, Tully T, and Quinn WG (1995). A Drosophila CREB/CREM homolog encodes multiple isoforms, including a cyclic AMP-dependent protein kinase-responsive transcriptional activator and antagonist. Mol. Cell. Biol 15, 5123–5130. [PubMed: 7651429]

Yin Y, Gao D, Wang Y, Wang Z-H, Wang X, Ye J, Wu D, Fang L, Pi G, Yang Y, et al. (2016). Tau accumulation induces synaptic impairment and memory deficit by calcineurin-mediated inactivation of nuclear CaMKIV/CREB signaling. Proc. Natl. Acad. Sci. USA 113, E3773–E3781. [PubMed: 27298345]

Zhang S-J, Zou M, Lu L, Lau D, Ditzel DAW, Delucinge-Vivier C, Aso Y, Descombes P, and Bading H (2009). Nuclear calcium signaling controls expression of a large gene pool: identification of a gene program for acquired neuroprotection induced by synaptic activity. PLoS Genet. 5, e1000604. [PubMed: 19680447]

Zhu LJ, Gazin C, Lawson ND, Pagès H, Lin SM, Lapointe DS, and Green MR (2010). ChIPpeakAnno: a Bioconductor package to annotate ChIP-seq and ChIP-chip data. BMC Bioinformatics 11, 237. [PubMed: 20459804]

Highlights

- Tau^{R406W} induces nuclear CREB depletion in neurons of the adult *Drosophila* brain

- Nuclear Ca^{2+} decreases with aging and tauopathy in the adult *Drosophila* brain

- Nuclear Ca^{2+} is depleted in iPSC-derived neurons from sporadic Alzheimer's disease

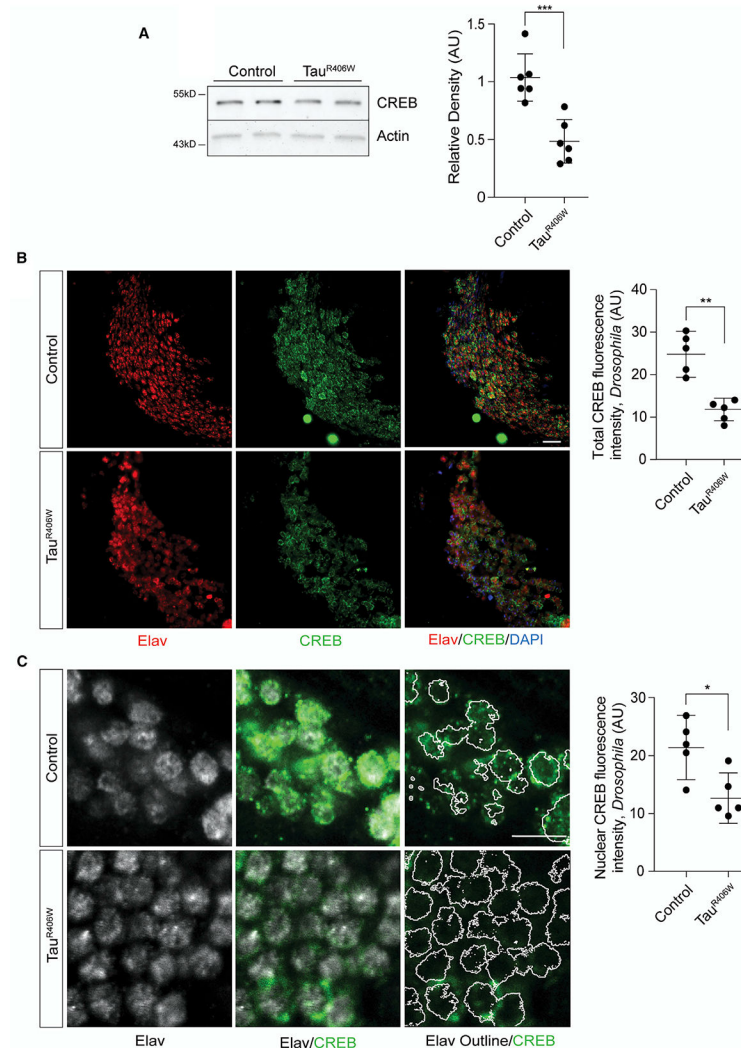- Pharmacologic/genetic manipulation of BK channels modify tau^{R406W} neurotoxicity

Figure 1. Tau^{R406W} Causes Reduction of Nuclear CREB in Neurons of the Adult *Drosophila* Brain

(A) CREB protein levels in control and tau^{R406W} transgenic *Drosophila* head lysates based on western blotting, n = 6 biological replicates.

(B) CREB and elav immunostaining in the mushroom body of control and tau^{R406W} transgenic *Drosophila* visualized by confocal microscopy. Images are from a single focal plane. n = 5 biological replicates. Scale bar, 5 μm.

(C) CREB and elav immunostaining in the mushroom body of control and tau^{R406W} transgenic *Drosophila* visualized by confocal microscopy. Images are from a single focal plane. Elav-based masks (represented by white outlines) were used to measure nuclear CREB levels, n = 5 biological replicates. Scale bar, 5 mm.

All assays were performed at day 10 of adulthood. Data are presented as mean ± SEM; unpaired t test; *p < 0.05, **p < 0.01, ***p < 0.001.
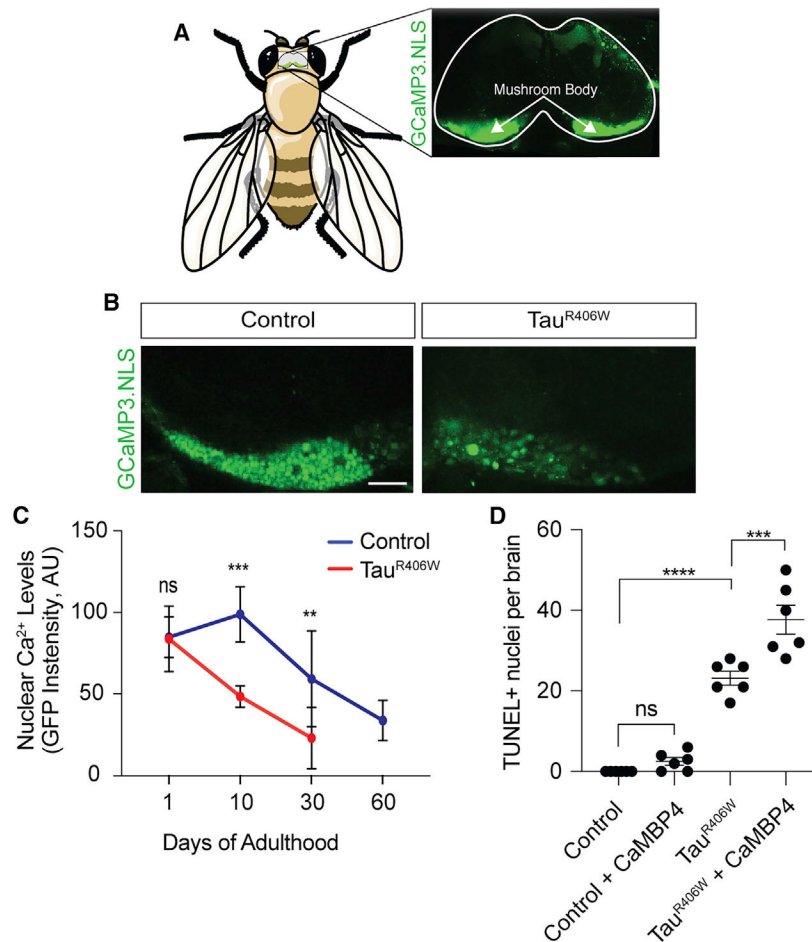
Figure 2. Tau^{R406W} Transgenic *Drosophila* Have a Toxic Reduction of Nuclear Ca^{2+}

(A) Activation of the nuclear Ca^{2+} reporter in the mushroom body of the adult *Drosophila* brain based on GCaMP3.NLS *in vivo* imaging.

(B) Decreased levels of nuclear Ca^{2+} in the mushroom body of the tau^{R406W} transgenic *Drosophila* brain versus control based on GCaMP3.NLS *in vivo* imaging. Images are of a single focal plane. Scale bar, 60 μm

(C) Quantification of nuclear Ca^{2+} based on GCaMP3.NLS in control and tau^{R406W} transgenic *Drosophila* of the indicated age. n = 6–8 biological replicates per genotype, per age. Data are presented as mean ± SD. For visual simplicity, significance is only noted for differences between genotypes at each age. Statistical analyses of the age-dependent decline in nuclear Ca^{2+} within each genotype are presented in Figures S1C and S1D.

(D) Neurodegeneration assayed by TUNEL staining in brains of control and tau^{R406W} transgenic *Drosophila* with and without nuclear Ca^{2+} blockage via panneuronal overexpression of CaMBP4.

All assays were performed at day 10 of adulthood with the exception of (C). Data are presented as mean ± SEM unless otherwise noted. One-way ANOVA with Tukey's multiple comparison test; ***p < 0.001, ****p < 0.0001.
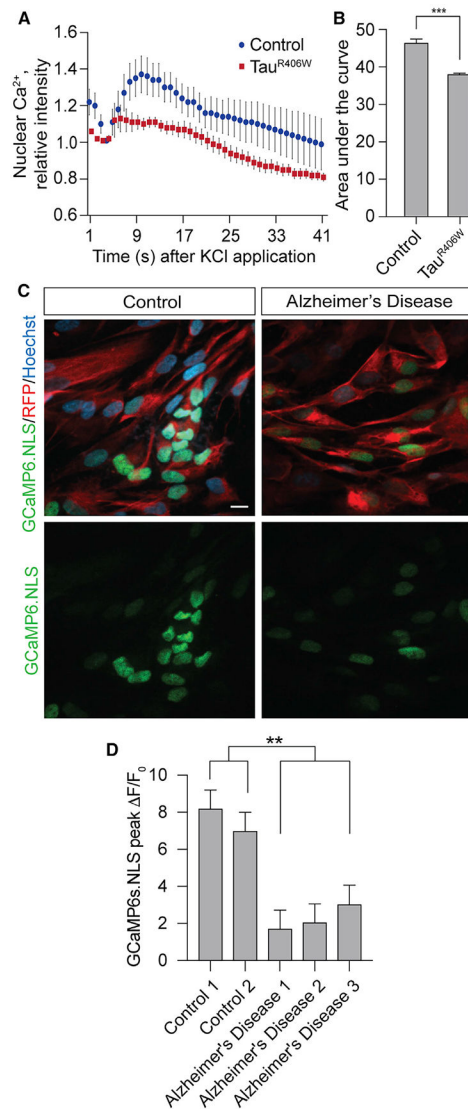
Figure 3. KCl-Induced Nuclear Ca^{2+} Influx Is Reduced in Brains of Tau^{R406W} Transgenic *Drosophila* and in iPSC-Derived Neurons from Sporadic Cases of Human Alzheimer's Disease

(A) Decreased depolarization-dependent influx of nuclear Ca^{2+} in tau^{R406W} transgenic *Drosophila* compared to control in response to administration of 70 mM KCl through a cuticular window in heads of living *Drosophila*.

(B) Quantification of the area under the curve from (A), n = 6 biological replicates.

(C) Decreased KCl-induced release of nuclear Ca^{2+} in iPSC-derived neurons from patients with Alzheimer's disease. Cells were transfected with membrane-bound RFP and the GCaMP6s.NLS nuclear Ca^{2+} reporter. Images show peak nuclear Ca^{2+} levels induced by 25 mM KCl. Images are from a single focal plane. Scale bar, 10 μm.

(D) Quantification of (C). Data are presented as peak ΔF/F$_0$, in which ΔF is the change in GCaMP6s.NLS GFP fluorescence, and F$_0$ is baseline GFP fluorescence. Nuclear Ca^{2+} was quantified in at least 50 single cells for each of six technical replicates per human sample. iPSC-derived neurons are from two control and three sporadic Alzheimer's disease patients.

All assays in *Drosophila* were performed at day 10 of adulthood. Data are presented as the mean ± SEM; unpaired t test or ANOVA; **p < 0.01, ***p < 0.001.
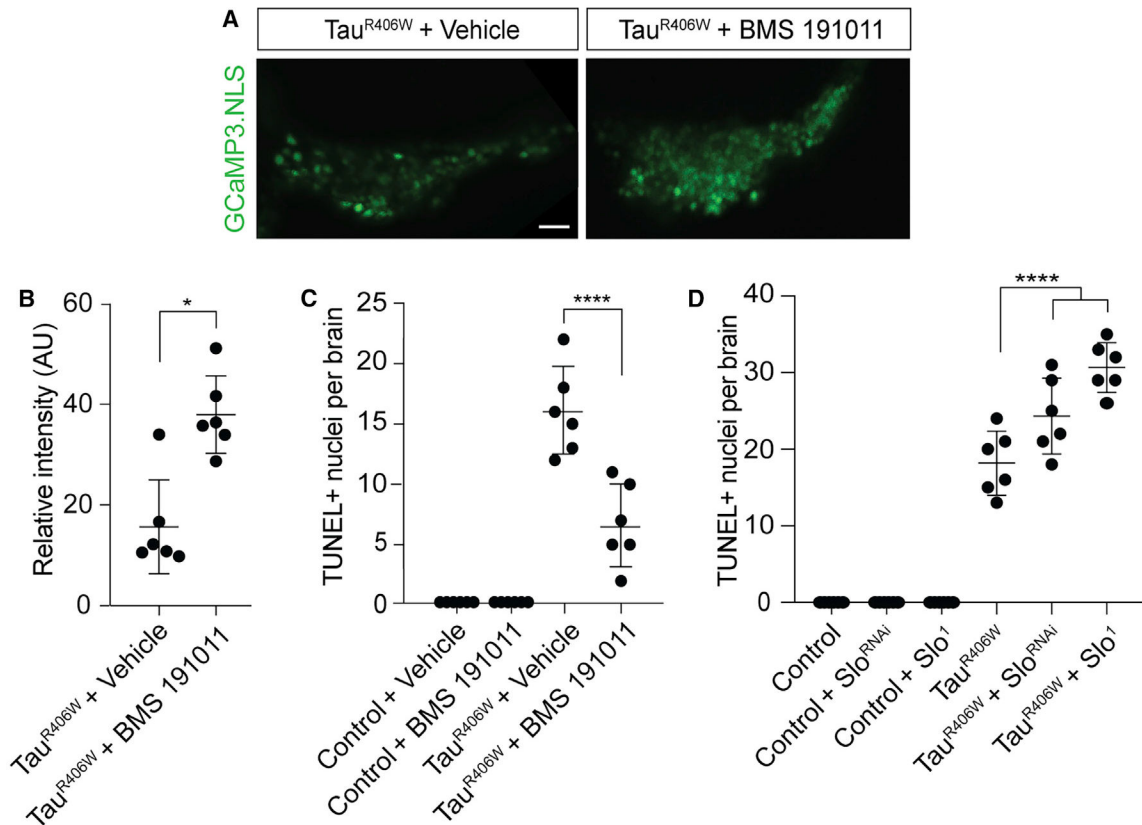
Figure 4. BK Channels Modify Nuclear Ca^{2+} Release and Neurotoxicity in Tau^{R406W} Transgenic *Drosophila*

(A) Visualization of nuclear Ca^{2+} based on *in vivo* imaging of GCaMP3.NLS in tau^{R406W} transgenic *Drosophila* fed either vehicle or BMS-191011 from days 2–10 of adulthood. Images are from a single focal plane. Scale bar, 10 μm.

(B) Quantification of (A), n = 6 biological replicates.

(C) Neurodegeneration assayed by TUNEL staining in the brains of control and tau^{R406W} transgenic *Drosophila* with and without exposure to BMS-191011 from days 2–10 of adulthood, n = 6 biological replicates.

(D) Neurodegeneration assayed by TUNEL staining in the brains of control and tau^{R406W} transgenic *Drosophila* with and without RNAi-mediated depletion or loss-of-function of *slowpoke*; n = 6 biological replicates.

All assays were performed at day 10 of adulthood. Data are presented as mean ± SEM; unpaired t test or ANOVA; *p < 0.05, ****p < 0.0001.

KEY RESOURCES TABLE

REAGENT or RESOURCE Antibodies	SOURCE	IDENTIFIER
Antobodies		
CREB	Cell Signaling	9197; RRID: AB_331277
Actin	Developmental Studies Hybridoma Bank	JLA20; RRID: AB_528068
Elav	Developmental Studies Hybridoma Bank	9F8A9; RRID: AB_528217
GFP	Thermo Fisher Scientific	CAB4211; RRID: AB_10709851
MAP2	Abcam	5392; RRID: AB_2138153
vGluT1	Abcam	Ab77822; RRID: AB_2187677
Chemicals, Peptides, and Recombinant Proteins		
BMS 191011	N/A	SML0866
Critical Commercial Assays		
TUNEL - FragEL DNA Fragmentation Detection Kit	EMD Millipore	QIA33
Ovation RNA-seq System for Drosophila	NuGen	0350
Clarity Max ECL Western Blotting Substrate	Bio-Rad	1705062
Deposited Data		
Control and tau^{R406W} RNA-seq data, day 10 of adulthood	GEO	GEO: GSE152278
Experimental Models: Cell Lines		
Control 1	Coriell Institute	GM25430; RRID: CVCL_1 N86
Control 2	Coriell Institute	GM27717
Alzheimer's Disease 1	Coriell Institute	CW50130; RRID: CVCL_JI63
Alzheimer's Disease 2	Coriell Institute	CW50136; RRID: CVCL_ER61
Alzheimer's Disease 3	Coriell Institute	CW50131; RRID: CVCL_HI88
Experimental Models: Organisms/Strains		
Elav-GAL4	Bloomington Drosophila Stock Center	458; RRID: BDSC_458
w1118	Bloomington Drosophila Stock Center	3605; RRID: BDSC_3605
UAS-tau^{R406W}	Dr. Mel Feany	Wittmann et al., 2001
UAS-GCaMP3.NLS	Dr. Hilmar Bading	Weislogel et al., 2013
UAS-CaMBP4	Dr. Hilmar Bading	Weislogel et al., 2013
Slo^{RNAi}	Bloomington Drosophila Stock Center	55405; RRID: BDSC_55405
Slo^1	Bloomington Drosophila Stock Center	4587; RRID: BDSC_4587
Software and Algorithms		
Trimmomatic	Bolger et al., 2014	v.0.36; RRID: SCR_011848
FastQC	http://www.bioinformatics.babraham.ac.uk/projects/fastqc/	RRID: SCR_014583
Salmon	Patro et al., 2017	v.0.13.1
DESeq2	Love et al., 2014	v1.24; RRID: SCR_015687
FlyBase - *Drosophila* transcriptome	Thurmond et al., 2019	FB2018_6.27; RRID: SCR_006549
FindM	Ambrosini et al., 2003	N/A

REAGENT or RESOURCE Antibodies	SOURCE	IDENTIFIER
Gene Expression Omnibus	Edgar et al., 2002	N/A; RRID: SCR_005012
ChlPpeakAnno	Zhuetal., 2010	N/A; RRID: SCR_012828
GraphPad Prism	GraphPad Software	Prism8; RRID: SCR_002798
Other		
CREB ChlP-seq dataset	Hirano et al., 2016	GEO: GSE73386, samples GSM1892406 and GSM1892408
Membrane-RFP plasmid	Addgene	57992; RRID: Addgene_57992
GCaMP6s.NLS plasmid	Dr. Hilmar Bading	Hagenston and Bading, 2011
BioT transfection reagent	Bioland Scientific	B01–01